Y. Chen, S. Lin, Z. Liang, N.C. Surawski, X. Huang (2022) *Smouldering Organic Waste Removal Technology with Smoke Emissions Cleaned by Self-Sustained Flame*, **Journal of Cleaner Production**, 362, 132363. https://doi.org/10.1016/j.jclepro.2022.132363

Smouldering Organic Waste Removal Technology with Smoke Emissions Cleaned by Self-Sustained Flame

Yuying Chen[1,3], Shaorun Lin[1,2], Zhirong Liang[1,*], Nicholas C. Surawski[3], and Xinyan Huang[1,*]

[1]*Research Centre for Fire Safety Engineering, The Hong Kong Polytechnic University, Hong Kong*

[2]*Hong Kong Polytechnic University Shenzhen Research Institute, Shenzhen, Guangdong, China*

[3]*School of Civil and Environmental Engineering, University of Technology Sydney, Sydney, Australia*

**Corresponding author: xy.huang@polyu.edu.hk* (XH); *zhirong.leung@outlook.com* (ZL)

Abstract

Smouldering is slow, low-temperature and flameless, and has been potentially regarded as an alternative for organic waste removal technology. However, as an incomplete combustion process, toxic smoke and pollutions from the smouldering are significant concerns that limit its popularization. This work applies a newly developed smouldering-based waste removal technology to investigate the removal of coffee waste, wood waste, and organic soil (simulated sludge) via using a flame to clean smouldering emissions at different airflow velocities (3-24 mm/s). Once ignited from the top, the smouldering front first propagates downwards where a stable flame situated above could be piloted and sustained to purify the smouldering emissions until the smouldering front reached the bottom of the fuel bed. The efficiency of pollution mitigation was demonstrated by significantly lower CO and VOCs emission after purification by self-sustained flame. The equivalent critical mass flux of flammable gases required for igniting the smouldering emissions is 0.5 g/m^2·s, regardless of the fuel type. The smouldering temperature, propagation rate and burning flux all increase with the airflow velocity but are also slightly sensitive to the type of waste. This work enriches strategies for the clean treatment of smouldering emissions and promotes an energy efficient and environmentally friendly method for organic waste removal.

Keywords: organic waste, smouldering combustion, flaming combustion, airflow velocity

1. Introduction

Smouldering is slow, low-temperature and flameless burning of porous fuels, which is a heterogeneous oxidative process sustained by the heat evolved when oxygen directly attacks a hot fuel surface and is different from flaming combustion in terms of transport processes and time scales (Ohlemiller, 1985; Rein, 2014). Once ignited, smouldering can survive in extreme conditions (e.g. with poor oxygen supply and high fuel moisture) and is the primary burning phenomenon of condensed-phase reactive porous media such as wood (Ohlemiller, 1991; Wang et al., 2021), incense (Lin et al., 2021), peat (Huang and Rein, 2016), cotton (Xie et al., 2020), and coal (Wu et al., 2015). Smouldering is the leading cause of casualties and injuries in residential fires, industrial fires and natural fires (Quintiere, 2006), but recent innovative developments (Hernandez-Soriano et al., 2016; Xin et al., 2021) have potentially revealed its wide application prospects.

In recent years, smouldering combustion has become one of the attractive alternatives for organic waste removal (Rashwan et al., 2021; Torero et al., 2020) that has been successfully applied in small- and large-scale tests to remove organic wastes with high moisture content like bioliquid (Kinsman et al., 2017; Zanoni et al., 2019), faces (Fabris et al., 2017; L. Yermán et al., 2017), wastewater sludge (Feng et al., 2021; Rashwan et al., 2021), and oil shale (Khan et al., 2020; Martins et al., 2010). For example, Yerman *et al.* (Rashwan et al., 2016; Yermán et al., 2015) showed that self-sustained smouldering could be achieved in faces with moisture contents up to 70%. Rahwan *et al.* (Rashwan et al., 2016) reported that robust smouldering in sludge could be sustained with a lower heating value of 1.6 MJ/kg. Also, many efforts have been also taken to improve the efficiency of smouldering-based waste removal technology, such as enhancing the oxygen supply (Pironi et al., 2009; Vantelon et al., 2005; L Yermán et al., 2017; Yermán et al., 2016) and adding sand to create a porous matrix (Switzer et al., 2014; L. Yermán et al., 2017).

On the other hand, toxic emissions from smouldering-based removal technology may pose severe threats to human health and environmental quality, which is a major public concern that limits its further promotion and application. Smoke produced by smouldering is mainly comprised of CO_2, CO, CH_4, HCN, NO_x, volatile organic compounds (VOCs) and particulate matter (PM) (Hu et al., 2018; Ravindra et al., 2019). Among them, CO_2 and CH_4 are the most significant greenhouse gases which accelerate the global warming. NO_x and VOCs (including a wide range of hydrocarbons, halocarbons and oxygenates) are the major precursors of O_3 and secondary organic aerosol (SOA) after complex photochemical processes (Urbanski et al., 2008). CO exposure can lead to health effects of human being, and even causes death. PMs emitted from smouldering, ranging from PM_1 to PM_{10}, is the key factor for causing haze episodes and can cause respiratory disease and induce cancer of people (Hu et al., 2018). Thus, with the fast-growing demand for clean environment and sustainable development, it is urgent to deepen our understanding and develop new strategies to mitigate the pollution of smouldering-based removal technology.

Considering that smouldering emissions are flammable, owing to the existence of large amounts of unburnt hydrocarbons, our previous work (see Fig. 1) has proposed a novel method to clean the toxic smoke via igniting these smouldering emissions (Chen et al., 2022). The flaming combustion that burn out smouldering emissions can co-exist with the smouldering combustion of solid wood wastes underneath, if the oxygen supply to both combustion modes are sufficient (Fig. 1c). However, whether the fuel type affects the

critical conditions and the efficiency for a flame to purify the smouldering emissions is still unknown, posing a significant knowledge gap.

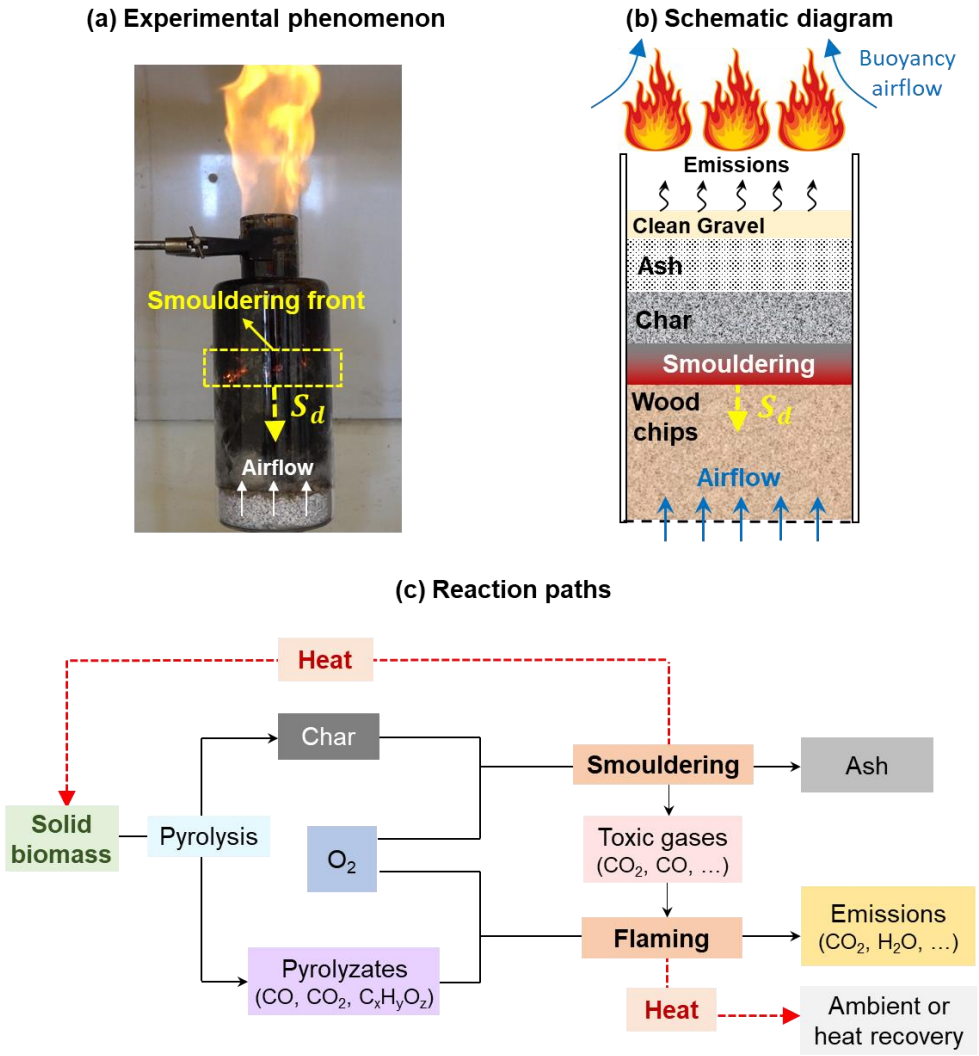

Fig. 1. Co-existence of smouldering and flaming of the wood waste (Chen et al., 2022).

Therefore, the main purpose of this study is to explore the impacts of fuel types on the smouldering characteristics and the critical conditions for maintaining a flame to purify the smouldering emissions. The experiments were conducted with three different organic wastes, including coffee waste, wood waste, and organic soil (simulated sludge) at airflow velocities from 3 mm/s to 24 mm/s. During the tests, smouldering emissions were measured with and without purification of flame to quantify the efficiency of pollution mitigation. The results obtained from this study will be helpful for the development of organic waste treatment by using smouldering combustion in an environmentally friendly and energy efficient way.

2. Methods

2.1. Organic waste samples

Wood waste, coffee waste and organic soil were selected as representative biowaste and food waste as well as simulated sludge, as shown in Fig. 2. Initially, all the fuel samples were oven-dried at 90 ^{o}C for 48 h, and their moisture contents were measured to be <8% when reaching a new equilibrium with ambient moisture.

The main properties of the three fuel samples are listed in Table 1, with clear differences in terms of density and particle size. In particular, the density of coffee waste is measured to be 420 kg/m^3, which is much larger than that of wood waste (200 kg/m^3) and organic soil (145 kg/m^3), while the particle size of it is the smallest, which is less than 1 mm (20-40 mm for wood waste and ~2 mm for organic soil).

Fig. 2. Photos of the organic waste samples used in experiments.

On the other hand, the volatile fraction of these three wastes only shows a slight difference, with the largest volatile fraction for coffee waste (80.1%) and the smallest fraction for organic soil (70.8%). In terms of elemental analysis, coffee waste had both the highest C/O ratio (1.45) and H/O ratio (0.21). The thermal analysis for all the samples was conducted with a PerkinElmer STA 6000 STA and the representative TG-DSC data are shown in Appendix (Fig. A1).

Table 1. Properties of the tested materials

Properties	Wood waste	Organic soil	Coffee waste
Bulk density (kg/m^3)	200±10	145±10	420±10
Particle size (mm)	20-40	~2	< 1
Volatile fraction (%)	78.4	70.8	80.1
Fixed carbon (%)	17.0	23.5	18.8
Ash (%)	4.6	5.7	1.1
C (%)	36.30	46.09	53.21
H (%)	3.73	5.75	7.72
O (%)	59.47	47.46	36.71
N (%)	0.44	0.47	2.01
S (%)	0.06	0.23	0.35
C/O	0.61	0.97	1.45
H/O	0.06	0.12	0.21

2.2. Experimental setup

The experimental setup was upgraded from our previous device (Chen et al., 2022), which included a cylindrical smouldering reactor, an electrical balance, an ignition system, an air supply system, and an emission test system, as illustrated in Fig. 3. The open-top reactor was made of 3-mm thick quartz glass, and it had a depth of 20 cm and an internal diameter of 10 cm. A 1 cm ceramic insulation layer was attached to the surface

of the reactor to reduce the heat losses. To straighten and homogenize the air supply from the bottom, a steel mesh was placed 3 cm above the bottom of the reactor, and a 2-cm gravel layer was poured onto the top surface of the steel mesh. Afterwards, a test sample was placed on the gravel layer with a constant height of 14 cm. To monitor the temperature and trace the position of the smouldering front, an array of five K-type thermocouples (1.5 mm bead diameter) was inserted into the fuel along the axis from 0 cm (bottom) to 12 cm (top) with an interval of 3 cm.

A coil heater buried 1 cm below the top of the fuel surface was used to initiate the smouldering combustion, and a lighter (as a pilot source) was installed at 2 cm above the outlet of the reactor to ignite the smouldering emissions. A forced airflow was supplied from the bottom end of the reactor, and the airflow rate was controlled by a flow meter. The experiments were performed at various airflow velocities (u) ranging from 3 mm/s to 24 mm/s.

The emissions were entirely collected using a fume extraction hood located above the reactor (Fig. 3). In the extraction hood, two measuring points were designed in the centreline of the hood duct. The flow rate in the test point was measured by an anemometer (Testo 405i), which was constant at 0.017 ± 0.005 m^3/s during the tests. Three different gas species were measured in this study: carbon dioxide (CO_2), carbon monoxide (CO), and volatile organic compounds (VOCs). After collecting the PM emissions using a quartz filter, CO and CO_2 were measured concurrently by a TSI 7575 Gas Analyzer, and the VOCs was measured by SKY2000 Portable Gas Analyzer.

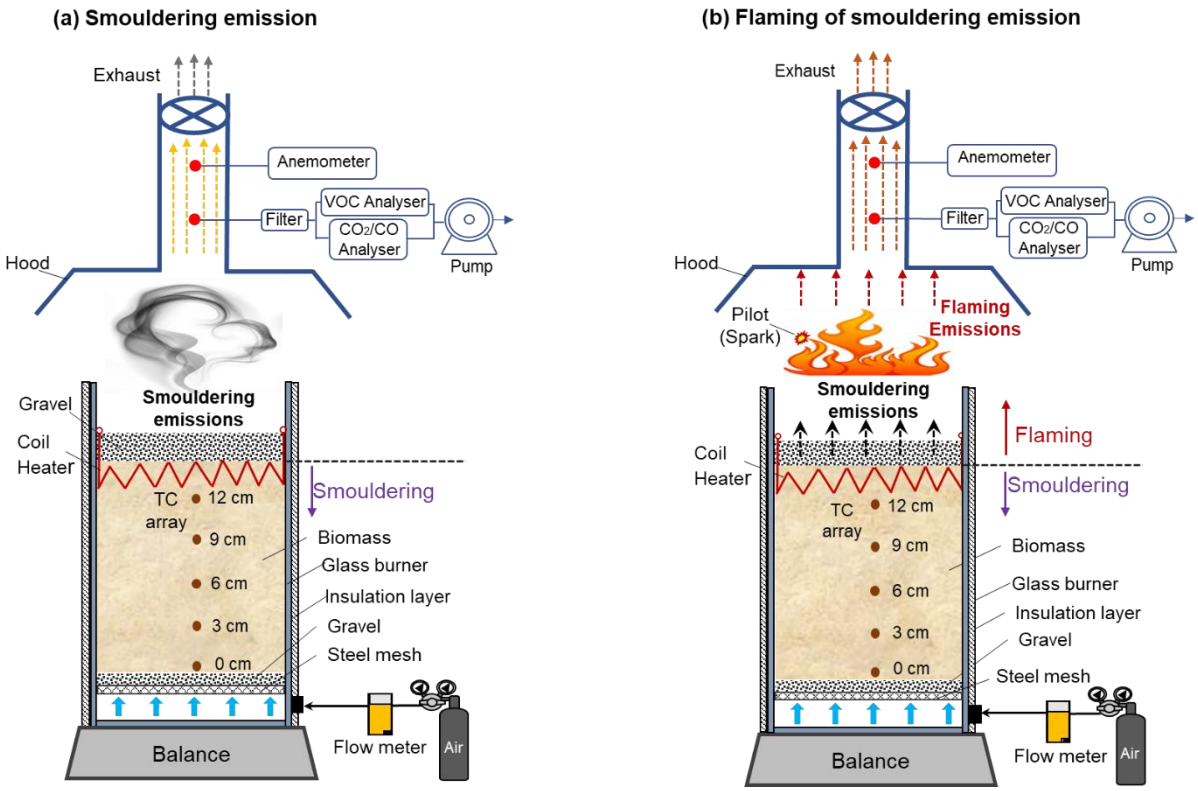

Fig. 3. Schematics of the experimental setups for (a) smouldering waste removal without smoke emission removal, and (b) smouldering waste removal with smoke emission removed by flame.

2.3. Experimental procedure

The ignition protocol involved setting the pilot heating rate to 100 W for 2 min, which was strong enough to initiate robust smouldering combustion of dry biomass. After forced ignition, a layer of fine and clean gravel with a height of 3 cm was placed on the fuel surface (Chen et al., 2022), and the forced airflow was fed from the bottom of the reactor with a prescribed flow velocity. As shown in Fig. 3a, the first group of experiments was conducted without the flame to quantify the characteristics of smouldering emissions, including both pyrolysis and char-oxidation emissions (see Fig. 1c). Afterward, a fresh sample was tested under the same airflow velocity, but a pilot source (lighter) was applied, aiming to ignite the smouldering emissions, as shown in Fig. 3b. Meanwhile, the emissions purified by the flame were also quantified and compared with those without flame purification.

All the experiments were stopped when all thermocouple measurements were below 200 °C. For each case, at least two tests were carried out to ensure the repeatability of the experiments. During tests, the ambient temperature (T_a) was 23 ± 2 °C, relative humidity was 50 ± 10%, and pressure was 1 atm.

3. Results and discussion

3.1. Phenomena of co-existence of smouldering and flaming

Fig. 4 shows an example of the combustion phenomenon of the wood waste at a large airflow velocity of 18 mm/s (see Video S1 in *Supplemental materials*). Similar to our previous findings (Chen et al., 2022), once ignited on the top, the smouldering front first propagated downward (1st stage, opposed). As the smouldering (glowing) front approached the fuel-bed bottom, it transitioned to the upward propagation (2nd stage, forward). More importantly, under such a large airflow velocity, the smouldering emissions from the 1st downward spread stage could be ignited and sustained a stable flame because the pyrolysis process dominated in this stage where a huge amount of flammable pyrolyzates were emitted. However, the flame can no longer be maintained at the 2nd stage until burnout because the pyrolysis process was almost finished at the first stage.

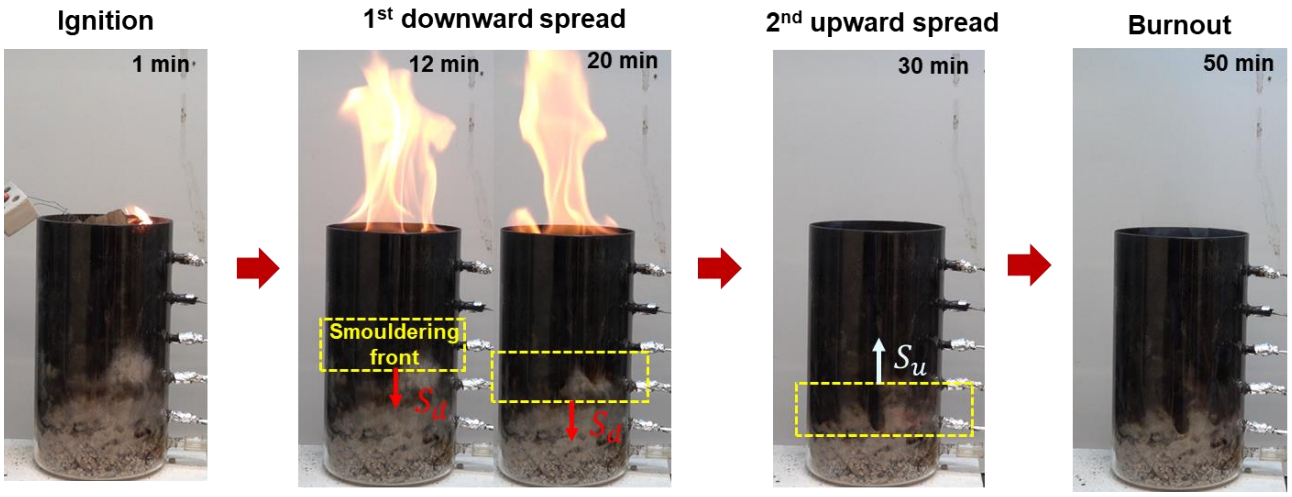

Fig. 4. Combustion phenomenon of wood waste with a bottom airflow velocity of u = 18 mm/s, where the reactor insulation is removed to observe the smouldering propagation.

3.2. Smouldering temperature and spread rate

Fig. 5 shows the smouldering temperature evolutions of wood waste, coffee waste, and organic soil at the airflow velocities of 18 mm/s. In general, the temperature profiles of different organic wastes are similar, showing two characteristic peak values. These two peaks correspond to the two smouldering stages as shown in Fig. 4, that is, 1st downward (opposed) spread, and 2nd upward (forward) spread. The peak temperature of the 1st stage ($T_{max,1}$) is usually lower than that of the 2nd stage ($T_{max,2}$), consistent with the major findings from previous studies (Huang and Rein, 2017; Lin and Huang, 2021). It is because fuel pyrolysis dominates the 1st stage, which is an endothermic process. Then, additional heat is required to maintain fast propagation of the flame front, as illustrated in Fig. 1c.

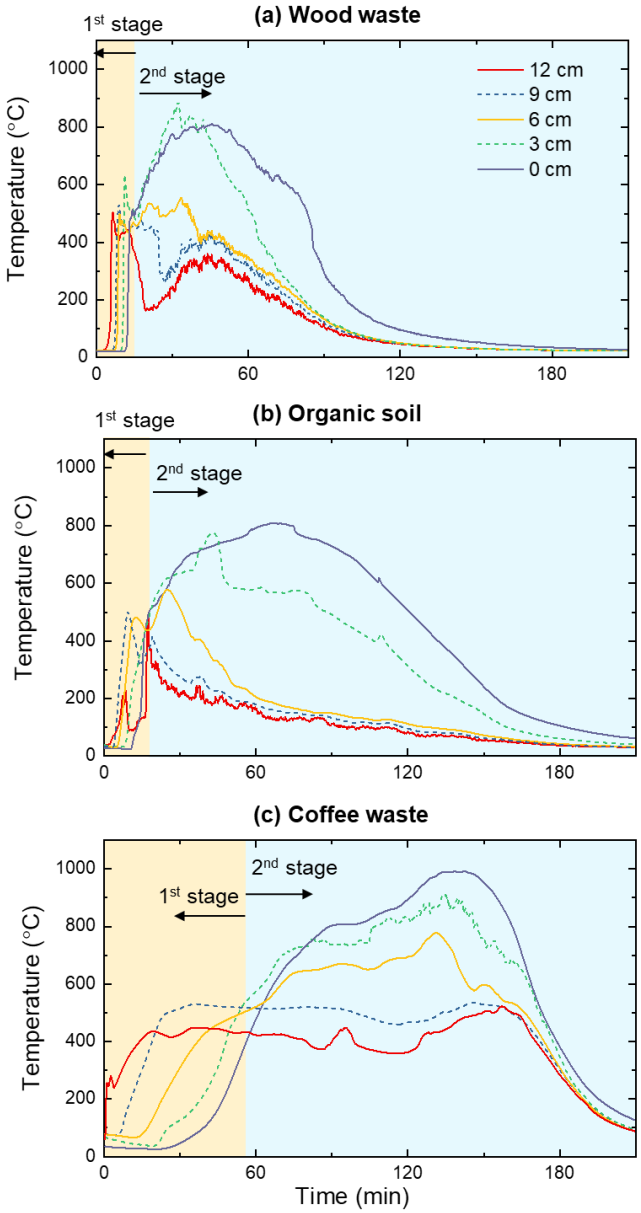

Fig. 5 Smouldering temperature profiles of (a) wood waste, (b) organic soil, and (c) coffee waste under the bottom airflow velocity of u = 18 mm/s.

After the pyrolysis front reaches the fuel bottom, only char oxidation exists, which is an exothermic process. Thus, higher temperatures can be observed. As airflow is applied from the bottom, the reaction front stays at

the bottom, and the fuel starts to regress with the burnout of the char. Therefore, at the 2nd stage, the temperature near the bottom is highest. Fig. 6a shows the mean peak temperatures of three organic wastes at two stages at different airflow velocities. Both peak temperatures increase with the airflow velocity because of stronger char oxidation, especially at the 2nd stage. Furthermore, the temperature was also found not to be extremely sensitive to waste types, where the peak temperatures of organic soil at both stages are slightly lower than those of the other two wastes. This may be because the density of organic soil is much smaller, causing less heat generated per fuel volume.

Fig. 6b shows the average spread rate of smouldering front versus airflow velocity. The average spread rate is calculated based on thermocouple readings. Specifically, the duration of 1st stage is determined by tracking the moments when the bottom thermocouple (0 cm) reaches its first peak temperature, while the duration of the 2nd stage is determined as the moments when all thermocouples are lower than 200 °C. As shown in Fig. 6a, for all the fuels, the smouldering spread rates at both smouldering stages increase with the airflow velocity. As the airflow velocity increases, the oxidation rate increases that accelerates both the heat-transfer and burning processes that promote the propagation of the smouldering front. More importantly, it was found that the smouldering spread rates of coffee waste are significantly lower than those of other wastes, especially at the 1st stage. This may be because of its smaller thermal diffusivity ($\alpha = k/\rho c$) resulting from a larger fuel density that could delay the rate of heat transfer (Incropera, 2007), thus slowing the propagation of the smouldering front.

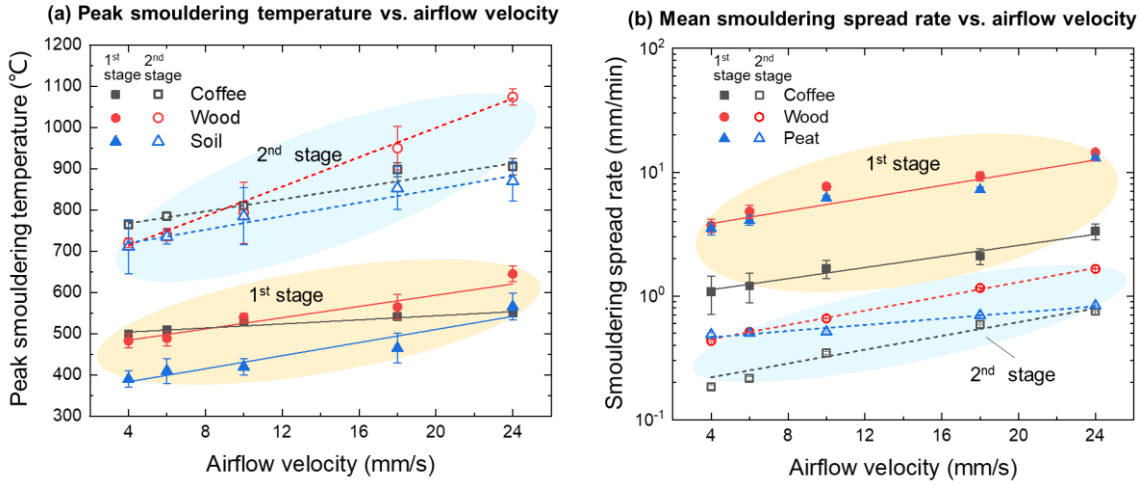

Fig. 6 (a) Peak smouldering temperatures and (b) average smouldering propagation rates of different organic wastes at two stages for different airflow velocities. Symbols show the experimental data (with standard deviations), lines are the manual fitting curves, yellow shading show the temperature and spread rate regions of the 1st stage, and blue shading show the temperature and spread rate regions of the 2nd stage

3.3. Smouldering burning flux

The smouldering burning flux ($\dot{m}''$) is the mass loss rate per unit area of the fuel, where the area of the fuel is determined by the inner diameter of the burner. These emission gases include both the pyrolysis gases and char-oxidation emissions, as illustrated in Fig. 1c. Fig. 7a-c shows the time evolution of the smouldering burning flux and remaining mass fraction of three organic wastes at a representative airflow velocity ($u =$

18 mm/s). The profiles of the burning flux of different organic wastes are similar: during the 1st stage, the burning flux increases rapidly, reaching a peak value. Afterwards, it dramatically decreases and remains stable at about 1-2 g/m^2·s during the 2nd stage until burnout occurs. For all the fuels, about 60%-70% of the mass is consumed at the 1st stage due to the release of pyrolyzates, consistent with the volatile contents reported in Table 1. Moreover, it can be found that the total fuel consumption through smouldering can reach over 90%.

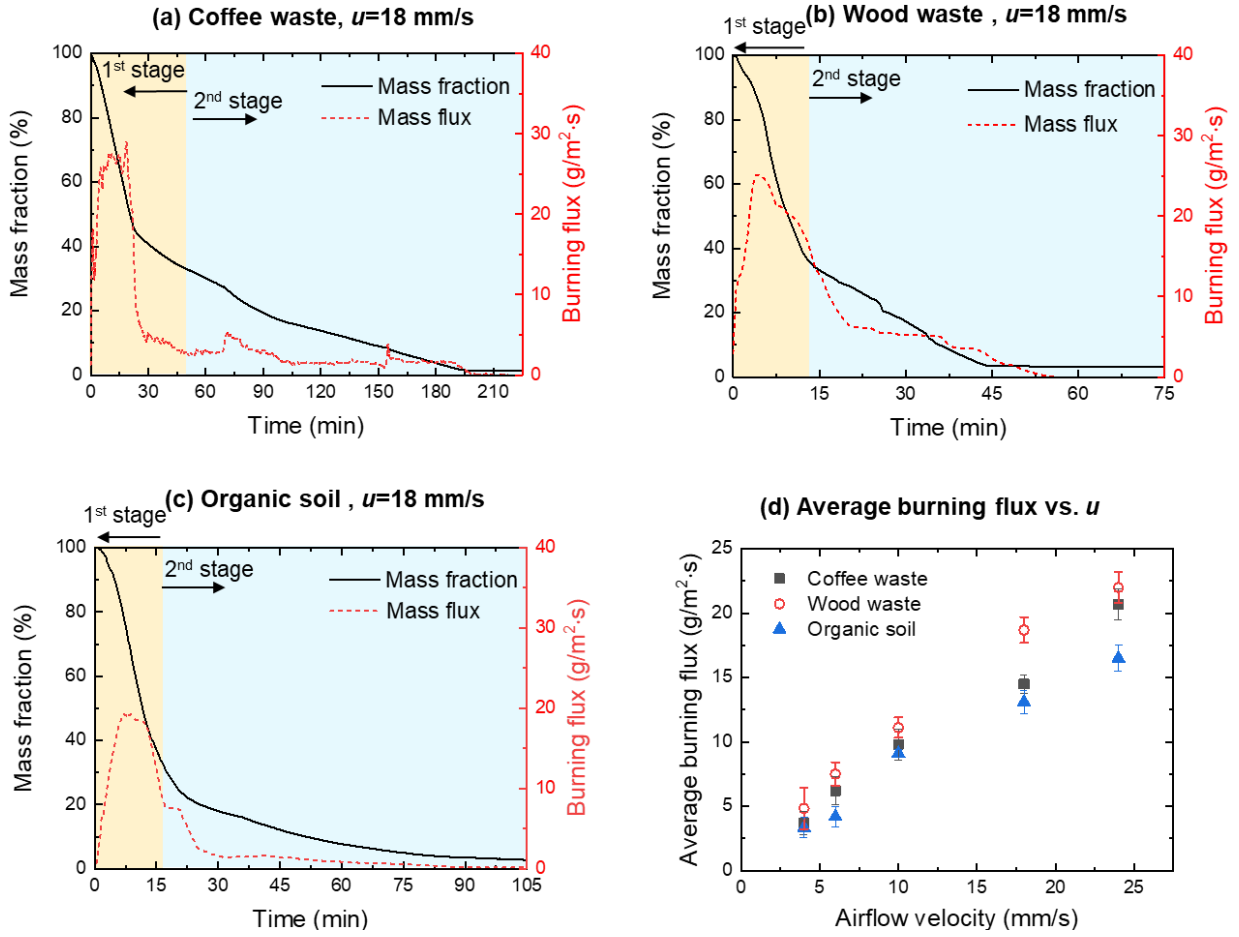

Fig. 7. Evolution of fuel mass fraction remaining and smouldering burning flux of (a) coffee waste, (b) wood waste, and (c) organic soil at the airflow velocity of 18 mm/s; and (d) the average smouldering burning flux versus the airflow velocity, where the error bars (SE $= \sigma/\sqrt{n}$, where n=2) show uncertainty of repeated tests.

Fig. 7d compares the average burning fluxes of different organic wastes at different airflow velocities. In general, the average burning flux increases with the airflow velocity. However, it can be observed that the average burning flux of wood waste is slightly larger under a certain airflow velocity, while the burning flux of organic soil is the smallest. For example, at $u = 24$ mm/s, the average burning flux of wood waste is 22 g/m^2·s, which is about 5 g/m^2·s greater than that of organic soil and 2 g/m^2·s larger than that of coffee waste.

Considering a 1-step global smouldering reaction, the smouldering burning flux ($\dot{m}''_F$) could be approximated as

$$\dot{m}''_F = \frac{\dot{m}''_{ox}}{v} = \frac{\rho_{ox} u}{v} = \rho_F S_{sm} \quad (1)$$

where $\dot{m}''_{ox}$ is the rate of oxygen supply, v is the stoichiometric coefficient, ρ_{ox} is the density of oxygen, u is the airflow rate, ρ_F is the density of fuel and S_{sm} is the smouldering propagation rate. Therefore, the smouldering burning flux increases as the airflow velocity increases, successfully explaining the increasing trend in Fig. 7d. Also, among these three organic wastes, Eq. (1) could also explain the maximum burning flux of wood waste, as it has a maximum smouldering propagation rate (see Fig. 6b) and moderate fuel density (Table 1).

3.4. Emissions characteristics

The mass flux of gas emissions ($\dot{m}''_i$, g/m^2 · s) is defined as the average mass flow rate per area (Hu et al., 2019). In this work, the transient mass fluxes of three gases: CO_2, CO, VOCs (mainly hydrocarbons), were calculated as

$$\dot{m}''_i(t) = \frac{\rho_i \Delta X_i(t) \dot{V} \times 10^{-3}}{A} \quad (2)$$

where ρ_i is the density of species i, which is calculated based on the assumptions of the ideal gas law (kg/m^3), $\Delta X_i(t)$ is the real-time concentration of the species i (ppm), which is calculated as $X_{i-plume} - X_{i-ambient}$, $\dot{V}$ is the volume flow rate in the duct (m^3/s), and A is the cross-sectional area of the smouldering burner (m^2).

Fig. 8a-c show the maximum mass fluxes of CO_2, CO, and VOCs from the smouldering of the three organic wastes at different airflow velocities, where the detailed time evolutions could be found in Fig. A2. In general, the maximum flux of each gas shows an increasing trend with the airflow velocity, and the mass flux of CO_2 is the largest among the three measured gases. Furthermore, at a certain airflow velocity, organic soil has a maximum mass flux of CO_2, but minimum mass fluxes for CO and VOCs. On the other hand, for coffee waste, it has a minimum mass flux of CO_2, but a maximum mass flux of VOCs.

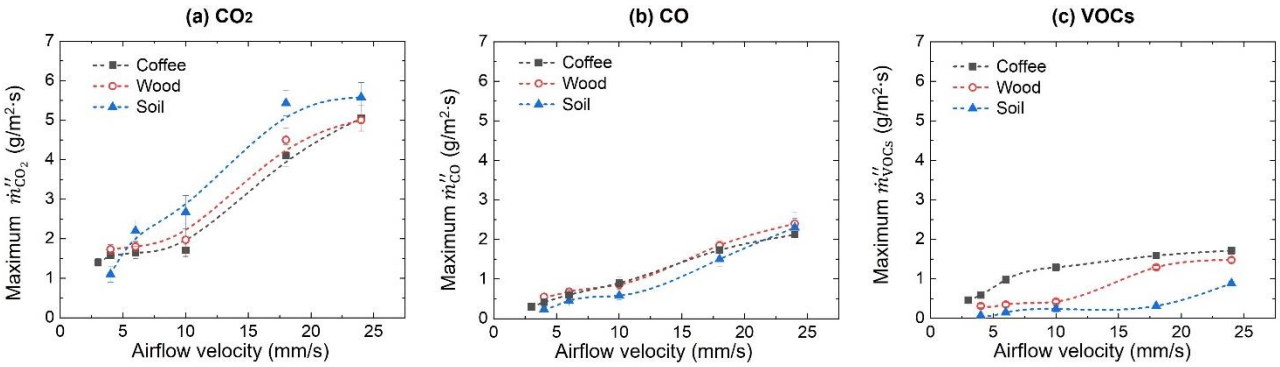

Fig. 8. Maximum mass flux of (a) CO_2, (b) CO, and (c) VOCs from the smouldering of different organic wastes at airflow velocities from 3-24 mm/s where the error bars (SE = $\sigma/\sqrt{n}$, where n=2) represent the standard deviations.

The $\Delta CO/\Delta CO_2$ ratio (also known as the modified combustion efficiency, which is expressed as MCE=$\Delta CO_2/(\Delta CO+\Delta CO_2)$) is an important index in describing combustion completeness (Hu et al., 2018), which can also indicate the type of pollutants emitted. Therefore, Fig. 9 further compares the $\Delta CO/\Delta CO_2$ ratios and MCE with and without the purification of flame to demonstrate the efficiency of pollution mitigation. Fig. 9a shows that the $\Delta CO/\Delta CO_2$ ratio for different organic wastes without flame purification is above 0.25.

However, if a flame is applied above the smouldering front, the $\Delta CO/\Delta CO_2$ ratio decreases dramatically to be below 0.05, which drops by more than 90%. Fig. 9b shows that the MCEs of smouldering for all organic wastes are lower than 0.8, while increasing to above 0.9 after a flame is supplied. Fig. 9c shows that in smouldering emission, $\Delta VOCs/\Delta CO_2$ ratios for all organic wastes are lower than 0.2. The production of VOCs from smouldering organic soil is much smaller, proving that its emission is much less flammable. On the other hand, with purification of flame, almost all VOCs is consumed in the flame, and the $\Delta VOCs/\Delta CO_2$ ratios in final emission are less than 0.0005. Therefore, this newly developed method can successfully alleviate the pollutions of the smouldering-based waste removal technology with a satisfactory efficiency of pollution mitigation.

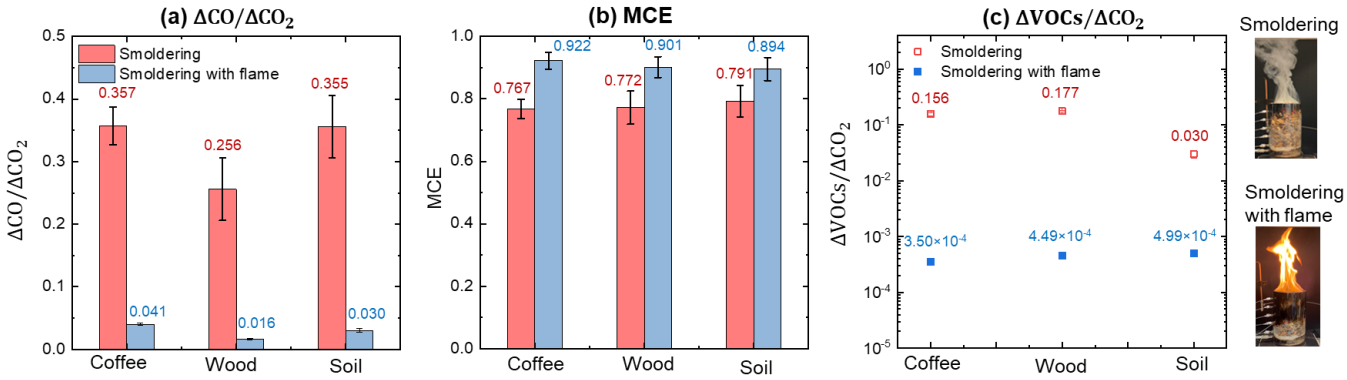

Fig. 9. Comparison of (a) $\Delta CO/\Delta CO_2$, (b) MCE, and (c) $\Delta VOCs/\Delta CO_2$ with and without flame purification at u=18 mm/s where the error bars (SE $= \sigma/\sqrt{n}$, where n=2) represent the standard deviations.

3.5. Criteria for sustaining a flame on the smouldering emissions

The first column of Fig. 10 shows the time evolution of the burning flux for coffee waste, wood waste, and organic soil under different airflow velocities. For all the organic wastes, the peak burning flux appears at the 1st stage under all airflow conditions. The second column of Fig. 10 further summarizes the maximum smouldering burning fluxes at different airflow velocities, as well as the minimum burning flux for maintaining a flame. Herein, the solid symbols represent the conditions where the flame can be piloted and co-exists with smouldering, while the hollow symbols signify the conditions where only smouldering can exist.

The minimum burning flux of coffee waste (Fig. 10b), wood waste (Fig. 10d), and organic soil (Fig. 10e) that is necessary to maintain a stable flame of their smouldering emissions are 7±1 g/m^2·s, 11±1 g/m^2·s, 17±2 g/m^2·s, where the minimum airflow velocities required to reach such a minimum burning flux are 3.5±0.5 mm/s, 6±0.5 mm/s, and 13.5±1.5 mm/s, respectively. Thus, with the smallest required burning flux and airflow velocity to sustain a flame, the smouldering emissions of coffee waste may be easier to be purified by this newly developed method.

Moreover, as shown in Fig. 10, the flame of the coffee waste emissions is dark orange, while the flame of the wood waste emissions is bright orange. However, the flame of the organic soil emissions is quite different from the other two fuels, which appears to be blue accompanied by red sparks. The red sparks are caused by the flaming of organic soil particles which are blown out by the airflow. The difference in the flame colour may be owing to the different flammable components that existed in their smouldering emissions.

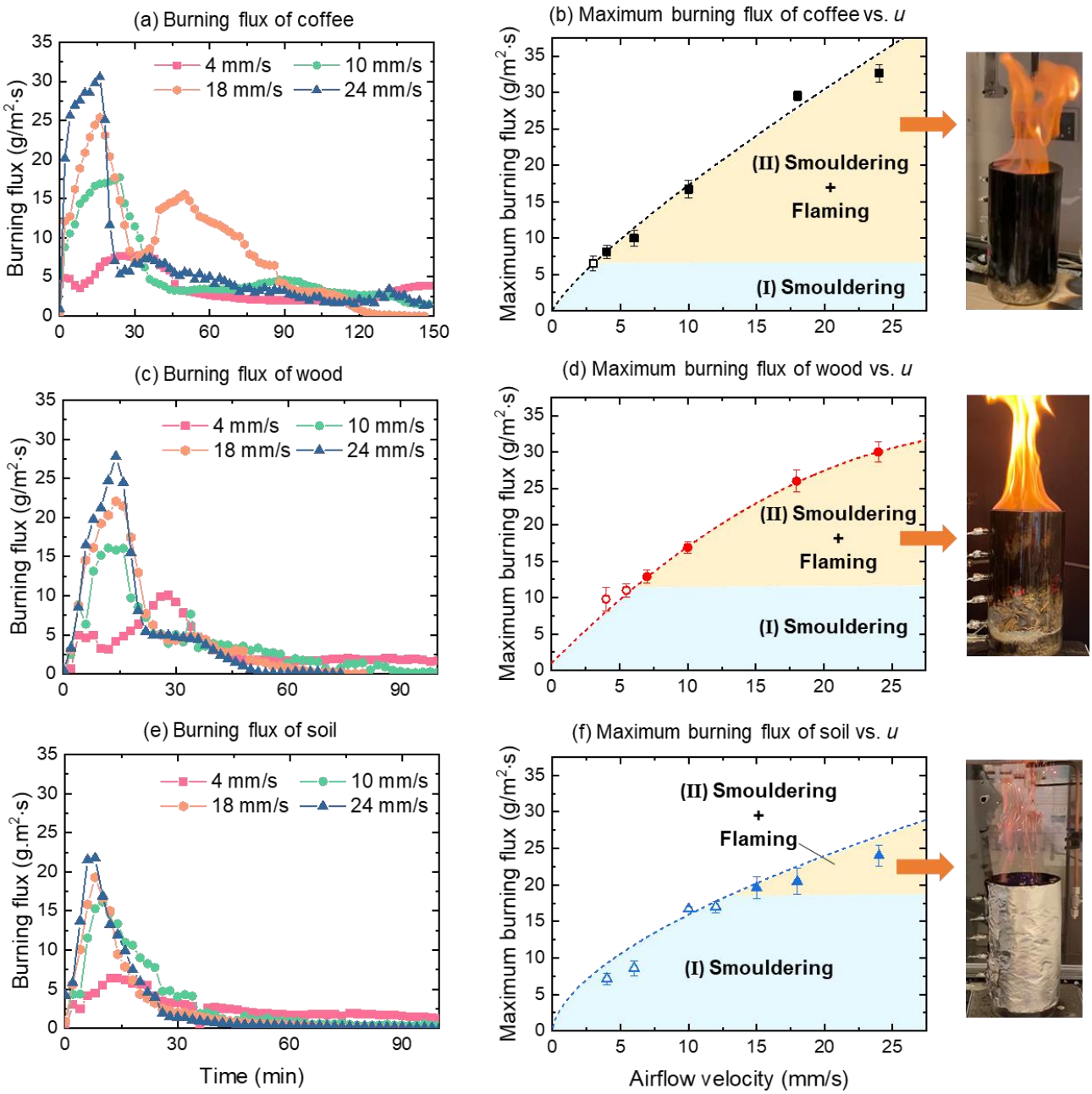

Fig. 10. Evolution of the burning flux for (a) coffee waste, (c) wood waste, and (e) organic soil under various airflow velocities. The maximum smouldering burning flux versus the airflow velocity of (b) coffee waste, (d) wood waste, and (f) organic soil, where the error bars (SE $= \sigma/\sqrt{n}$, where n=2) show test uncertainty.

To ignite and maintain a flame, a minimum mass flux of fuel gas is required. In this study, the fuel gas in the smouldering emissions is simplified to a mixture of VOCs (mainly hydrocarbons) and carbon monoxide (CO), which have been proved to be the main flammable gas species in the smouldering emissions (Hu et al., 2020, 2019). Thus, the equivalent mass flux of flammable gas emissions ($\dot{m}_f''$) becomes

$$\dot{m}_f'' = \frac{\Delta H_{\mathrm{HC}} \cdot \dot{m}_{\mathrm{HC}}'' + \Delta H_{\mathrm{CO}} \cdot \dot{m}_{\mathrm{CO}}''}{\Delta H_{\mathrm{HC}}} \tag{3}$$

where ΔH_{HC} is the heat of combustion of hydrocarbons, ΔH_{CO} is the heat of combustion of CO, $\dot{m}_{\mathrm{HC}}''$ and $\dot{m}_{\mathrm{CO}}''$ are the mass fluxes of hydrocarbons and CO, respectively.

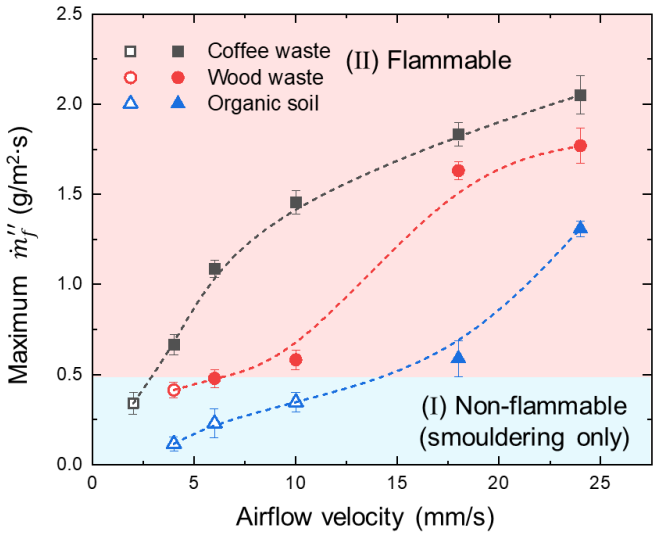

Fig. 11. The maximum mass flux of flammable components in smouldering emissions versus the airflow velocity, where the error bars (SE $= \sigma/\sqrt{n}$, where n=2) show the experimental uncertainty of repeated tests.

Fig. 11 summarizes the maximum mass flux of flammable gas emissions from three different organic wastes at different airflow velocities. For each organic waste, the maximum $\dot{m}_f''$ increases with airflow velocity (u). The $\dot{m}_f''$ of coffee waste is the largest, while the $\dot{m}_f''$ of organic soil is the smallest. For example, as the airflow velocity increases from 4 to 24 mm/s, the maximum $\dot{m}_f''$ of coffee waste increases from 0.68 to 2.2 g/m^2·s, while the maximum $\dot{m}_f''$ of organic soil increases from 0.11 to 1.27 g/m^2·s. More importantly, the minimum mass flux of flammable gas emissions ($\dot{m}_{f,crt}''$) of about 5 g/m^2·s could be found to sustain a flame of the emissions. To reach such a critical mass flux, a much larger airflow velocity smouldering (about 14 mm/s) is required for organic soil compared with another two organic wastes. These consistent with the critical airflow velocity we observed in Fig. 10.

4. Conclusions

In this work, we successfully apply a newly developed method to purify the toxic and pollutant emissions from the smouldering-based removal of coffee waste, wood waste and simulated sludge (organic soil) via igniting a flame above the smouldering front. Once the smouldering front is ignited from the top fuel surface, it first propagates downwards to the fuel-bed bottom and then propagates upwards. The flame could only be piloted and self-sustained at the 1st stage owing to an intense pyrolysis process. The efficiency of pollution mitigation is demonstrated by significantly lower CO and VOCs emission (with $\Delta CO/\Delta CO_2$<0.05 and $\Delta VOCs/\Delta CO_2$ <0.0005) after purification by self-sustained flame. The equivalent critical mass flux of flammable gases required for igniting the smouldering emissions is 0.5 g/m^2·s, regardless of biomass fuel types.

The smouldering temperature, propagation rate and burning flux are all increased with the airflow velocity but are also slightly sensitive to the fuel type. This work demonstrates the applicability of this newly developed waste removal technology and demonstrates its efficiency of pollution mitigation, thus further enriching strategies for the clean treatment of smouldering emissions and promoting an energy-efficient and environmentally friendly method for biowaste removal. Future work will determine the effect of fuel moisture content and operational conditions on the critical conditions of flame purification.

CRediT authorship contribution statement

Yuying Chen: Investigation, Writing-original draft, Formal analysis. **Shaorun Lin:** Formal analysis, Writing-review & editing, Resources. **Zhirong Liang:** Investigation, Formal analysis, Resources. **Nicholas C. Surawski:** Supervision, Writing-review & editing. **Xinyan Huang:** Conceptualization, Supervision, Writing-review & editing, Funding acquisition.

Declaration of Competing Interest

The authors declare that there is no conflict of interest

Acknowledgments

This work is funded by the National Natural Science Foundation of China (NSFC grant No. 51876183), ZJU SKLCEU Open Fund (2018012), Sichuan Science and Technology Program (2019YFSY0040), and Society of Fire Protection Engineers (SFPE) Educational & Scientific Foundation.

References

Chen, Y., Liang, Z., Lin, S., Huang, X., 2022. Limits of sustaining a flame above smoldering woody biomass. Combustion Science and Technology 00, 1–19. https://doi.org/10.1080/00102202.2022.2041000

Fabris, I., Cormier, D., Gerhard, J.I., Bartczak, T., Kortschot, M., Torero, J.L., Cheng, Y.-L., 2017. Continuous, self-sustaining smouldering destruction of simulated faeces. Fuel 190, 58–66.

Feng, C., Huang, J., Yang, C., Li, C., Luo, X., Gao, X., Qiao, Y., 2021. Smouldering combustion of sewage sludge: Volumetric scale-up, product characterization, and economic analysis. Fuel 305, 121485. https://doi.org/10.1016/j.fuel.2021.121485

Hernandez-Soriano, M.C., Kerré, B., Kopittke, P.M., Horemans, B., Smolders, E., 2016. Biochar affects carbon composition and stability in soil: A combined spectroscopy-microscopy study. Scientific Reports 6, 1–13. https://doi.org/10.1038/srep25127

Hu, Y., Christensen, E., Restuccia, F., Rein, G., 2019. Transient gas and particle emissions from smouldering combustion of peat. Proceedings of the Combustion Institute 37, 4035–4042. https://doi.org/10.1016/j.proci.2018.06.008

Hu, Y., Cui, W., Rein, G., 2020. Haze emissions from smouldering peat: The roles of inorganic content and bulk density. Fire Safety Journal 113, 102940. https://doi.org/10.1016/j.firesaf.2019.102940

Hu, Y., Fernandez-Anez, N., Smith, T.E.L., Rein, G., 2018. Review of emissions from smouldering peat fires and their contribution to regional haze episodes. International Journal of Wildland Fire 27(5), 293. https://doi.org/10.1071/WF17084

Huang, X., Rein, G., 2017. Downward spread of smouldering peat fire: The role of moisture, density and oxygen supply. International Journal of Wildland Fire 26, 907–918. https://doi.org/10.1071/WF16198

Huang, X., Rein, G., 2016. Interactions of Earth's atmospheric oxygen and fuel moisture in smouldering wildfires. Science of the Total Environment 572, 1440–1446. https://doi.org/10.1016/j.scitotenv.2016.02.201

Incropera, F.P., 2007. Principles of heat and mass transfer, Fundamentals of Heat and Mass Transfer. John Wiley.

Khan, M.A., Alqadami, A.A., Wabaidur, S.M., Siddiqui, M.R., Jeon, B.-H., Alshareef, S.A., Alothman, Z.A., Hamedelniel, A.E., 2020. Oil industry waste based non-magnetic and magnetic hydrochar to sequester potentially toxic post-transition metal ions from water. Journal of Hazardous Materials 400, 123247. https://doi.org/https://doi.org/10.1016/j.jhazmat.2020.123247

Kinsman, L., Torero, J.L., Gerhard, J.I., 2017. Organic liquid mobility induced by smoldering remediation. Journal of Hazardous Materials 325, 101–112. https://doi.org/https://doi.org/10.1016/j.jhazmat.2016.11.049

Lin, S., Chow, T.H., Huang, X., 2021. Smoldering propagation and blow-off on consolidated fuel under external airflow. Combustion and Flame 234, 111685. https://doi.org/10.1016/j.combustflame.2021.111685

Lin, S., Huang, X., 2021. Quenching of Smoldering: Effect of Wall Cooling on Extinction. Proceedings of the Combustion Institute (Accepted) 38.

Martins, M.F., Salvador, S., Thovert, J.-F., Debenest, G., 2010. Co-current combustion of oil shale – Part 1: Characterization of the solid and gaseous products. Fuel 89, 144–151. https://doi.org/10.1016/j.fuel.2009.06.036

Ohlemiller, T.J., 1991. Smoldering Combustion Propagation On Solid Wood. Fire Safety Science 3, 565–574. https://doi.org/10.3801/IAFSS.FSS.3-565

Ohlemiller, T.J., 1985. Modeling of smoldering combustion propagation. Progress in Energy and Combustion Science 11, 277–310. https://doi.org/https://doi.org/10.1016/0360-1285(85)90004-8

Pironi, P., Switzer, C., Rein, G., Fuentes, A., Gerhard, J.I., Torero, J.L., 2009. Small-scale forward smouldering experiments for remediation of coal tar in inert media. PROCEEDINGS OF THE COMBUSTION INSTITUTE 32, 1957–1964. https://doi.org/10.1016/j.proci.2008.06.184

Quintiere, J.G., 2006. Fundamentals of fire phenomena, Fundamentals of Fire Phenomena. John Wiley. https://doi.org/10.1002/0470091150

Rashwan, T.L., Fournie, T., Torero, L., Grant, G.P., Gerhard, J.I., 2021. Scaling up self-sustained smouldering of sewage sludge for waste-to-energy Distance 135, 298–308. https://doi.org/10.1016/j.wasman.2021.09.004

Rashwan, T.L., Gerhard, J.I., Grant, G.P., 2016. Application of self-sustaining smouldering combustion for the destruction of wastewater biosolids. Waste Management 50, 201–212. https://doi.org/10.1016/j.wasman.2016.01.037

Ravindra, K., Singh, T., Mor, S., 2019. Emissions of air pollutants from primary crop residue burning in India and their mitigation strategies for cleaner emissions. Journal of Cleaner Production 208, 261–273. https://doi.org/https://doi.org/10.1016/j.jclepro.2018.10.031

Rein, G., 2014. Smoldering Combustion. SFPE Handbook of Fire Protection Engineering 2014, 581–603. https://doi.org/10.1007/978-1-4939-2565-0_19

Switzer, C., Pironi, P., Gerhard, J.I., Rein, G., Torero, J.L., 2014. Volumetric scale-up of smouldering

remediation of contaminated materials. Journal of Hazardous materials 268, 51–60.

Torero, J.L., Gerhard, J.I., Martins, M.F., Zanoni, M.A.B., Rashwan, T.L., Brown, J.K., 2020. Processes defining smouldering combustion: Integrated review and synthesis. Progress in Energy and Combustion Science 81. https://doi.org/10.1016/j.pecs.2020.100869

Urbanski, S.P., Hao, W.M., Baker, S., 2008. Chapter 4 Chemical Composition of Wildland Fire Emissions. Developments in Environmental Science 8, 79–107. https://doi.org/10.1016/S1474-8177(08)00004-1

Vantelon, J.-P., Lodeho, B., Pignoux, S., Ellzey, J.L., Torero, J.L., 2005. Experimental observations on the thermal degradation of a porous bed of tires. Proceedings of the Combustion Institute 30, 2239–2246. https://doi.org/https://doi.org/10.1016/j.proci.2004.08.109

Wang, S., Ding, P., Lin, S., Huang, X., Usmani, A., 2021. Deformation of wood slice in fire: Interactions between heterogeneous chemistry and thermomechanical stress. Proceedings of the Combustion Institute 38, 5081–5090. https://doi.org/10.1016/j.proci.2020.08.060

Wu, D., Huang, X., Norman, F., Verplaetsen, F., Berghmans, J., Van den Bulck, E., 2015. Experimental investigation on the self-ignition behaviour of coal dust accumulations in oxy-fuel combustion system. Fuel 160, 245–254. https://doi.org/10.1016/j.fuel.2015.07.050

Xie, Q., Zhang, Z., Lin, S., Qu, Y., Huang, X., 2020. Smoldering Fire of High-Density Cotton Bale Under Concurrent Wind. Fire Technology 56, 2241–2256. https://doi.org/10.1007/s10694-020-00975-1

Xin, X., Dell, K., Udugama, I.A., Young, B.R., Baroutian, S., 2021. Transforming biomass pyrolysis technologies to produce liquid smoke food flavouring. Journal of Cleaner Production 294, 125368. https://doi.org/https://doi.org/10.1016/j.jclepro.2020.125368

Yermán, L, Cormier, D., Fabris, I., Carrascal, J., Torero, J.L., Gerhard, J.I., Cheng, Y.-L., 2017. Potential bio-oil production from smouldering combustion of faeces. Waste and biomass valorization 8, 329–338.

Yermán, L., Hadden, R.M., Carrascal, J., Fabris, I., Cormier, D., Torero, J.L., Gerhard, J.I., Krajcovic, M., Pironi, P., Cheng, Y.-L., 2015. Smouldering combustion as a treatment technology for faeces: exploring the parameter space. Fuel 147, 108–116.

Yermán, L., Wall, H., Torero, J., Gerhard, J.I., Cheng, Y.L., 2016. Smoldering Combustion as a Treatment Technology for Feces: Sensitivity to Key Parameters. Combustion Science and Technology 188, 968–981. https://doi.org/10.1080/00102202.2015.1136299

Yermán, L., Wall, H., Torero, J.L., 2017. Experimental investigation on the destruction rates of organic waste with high moisture content by means of self-sustained smoldering combustion. Proceedings of the Combustion Institute 36, 4419–4426. https://doi.org/10.1016/j.proci.2016.07.052

Zanoni, M.A.B., Torero, J.L., Gerhard, J.I., 2019. The role of local thermal non-equilibrium in modelling smouldering combustion of organic liquids. Proceedings of the Combustion Institute 37, 3109–3117. https://doi.org/https://doi.org/10.1016/j.proci.2018.05.177

Appendix

Three diverse kinds of samples were pulverized into powders and dried at 90 °C for 48 h. The TG-DSC test was conducted with a PerkinElmer STA 6000 Simultaneous Thermal Analyzer. The initial mass was about 2-3 mg, and samples were heated at the constant rates of 30 K/min. Two oxygen concentrations were selected, 0% (nitrogen) and 21% (air) with a flow rate of 20 mL/min. Experiments were repeated twice for each case, and good repeatability is shown. Fig. A1 shows the mass fraction, mass loss rate, and heat flow curves of (a) wood waste, (b) organic soil, and (c) coffee waste. From the mass-fraction (TG) curves, it can be observed that the pyrolysis could consume nearly 70% of the fuel. The heat of smouldering (ΔH_{sm}) can be calculated by integrating the heat flow curve, which are 23.6 MJ/kg, 25.7 MJ/kg, and 33.4 MJ/kg for wood waste, organic soil, and coffee waste, respectively.

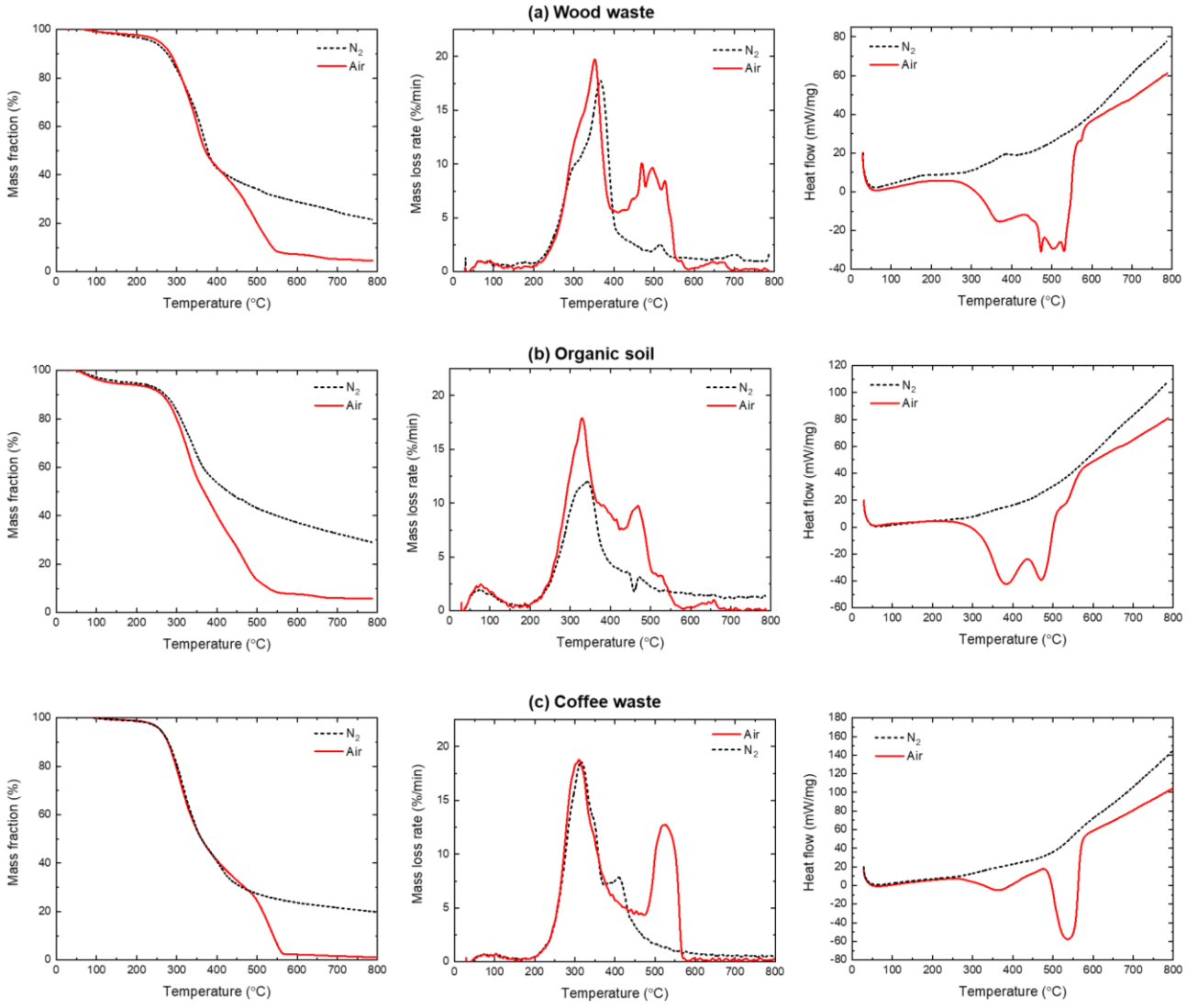

Fig. A1 TGA-DSC results of (a) wood waste, (b) organic soil, and (c) organic waste at a heating rate of 30 K/min.

Fig. A2 shows the evolution of the transient mass flux of CO_2, CO, and VOCs from the smouldering of different organic wastes at a representative airflow velocity of 18 mm/s. The mass fluxes of gas species peak at the 1st smouldering stage where 60% fuel mass is consumed, as shown in Fig. 7.

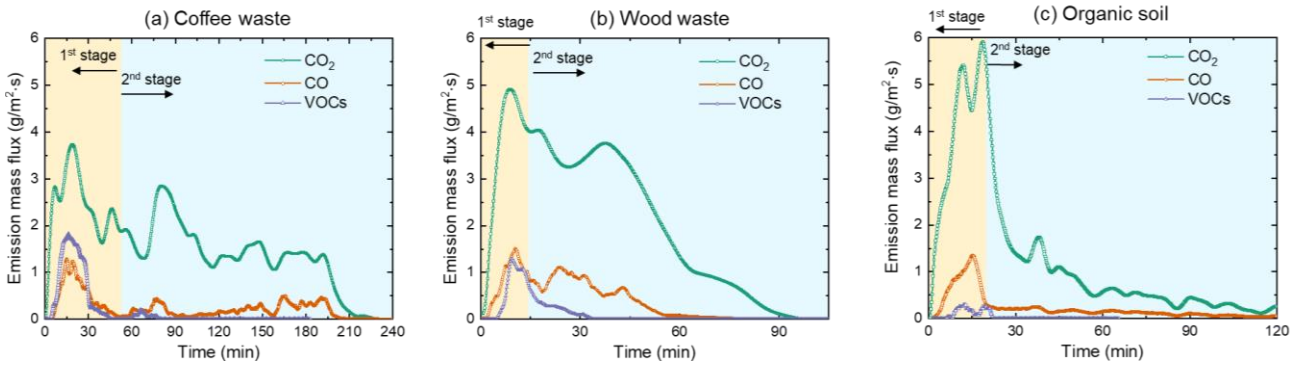

Fig. A2 Evolution of mass flux of gas species from smouldering of (a) coffee waste, (b) wood waste, and (c) organic soil at u=18 mm/s.

The transient emission factor (EF_i, g/kg) for gas species is calculated through Eq. (A1)

$$EF_i(t) = \frac{\dot{m}_i''(t)}{\dot{m}''(t)} \times 10^3 \quad \text{(A1)}$$

where $\dot{m}''(t)$ is the fuel burning flux shown in ***Section 3.3***., and $\dot{m}_i''(t)$ is the mass flux of smouldering gas emissions shown in ***Section 3.4***.

Fig. A3 shows the time evolutions of emission factors of CO_2, CO, and VOCs under two representative airflow velocities of 4 mm/s and 18 mm/s. Generally, the EFs of all gas species increase dramatically with the airflow velocity. Taking organic soil as an example, the maximum EF of CO_2 increases from 1300 to 3000 g/kg as the airflow velocity increases from 4 to 18 mm/s. EFs of CO_2 and CO show a similar increasing trend with time, both of which are small during the 1st stage and increase at the 2nd stage. For example, as shown in Fig. A3(c), the average EF of organic soil during the 1st stage is about 50 g/kg and increases to about 200 g/kg at the 2nd stage. Moreover, both EFs of CO_2 and CO increase dramatically in the burnout stage, which is due to the rapid decrease of the $\dot{m}''(t)$. The evolution of the EF of VOCs is quite different from that of CO_2 and CO. Fig. A3(e, f) show that EF of VOCs usually peaks at the 1st stage which is dominated by fuel pyrolysis. Comparatively, the wood waste and organic soil have larger EFs of CO_2 and CO than coffee waste, while coffee waste has a much larger EF-VOCs. For example, the EF-VOCs of coffee waste can reach about 250 g/kg at u=18 mm/s, which is 10 times that of organic soil.

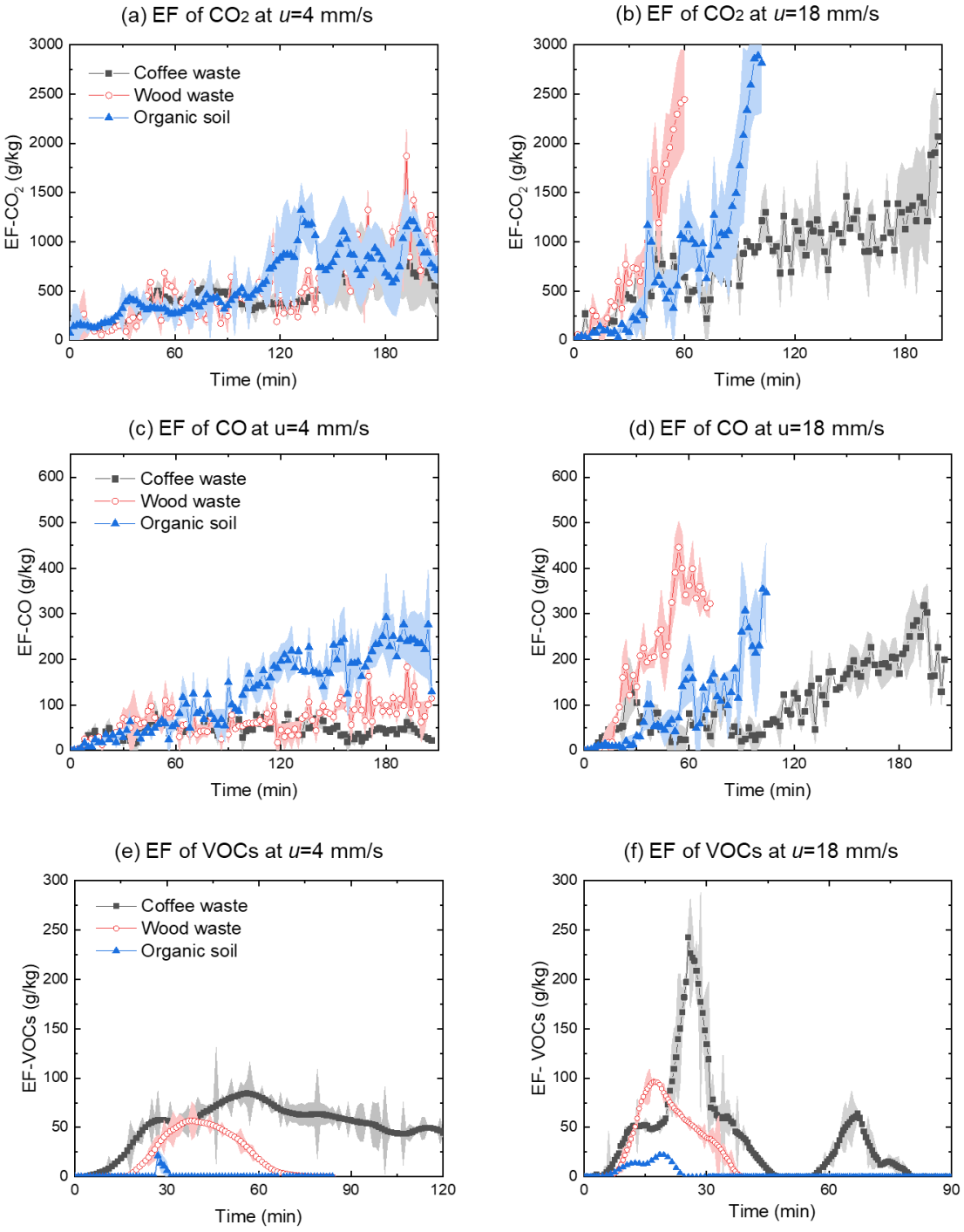

Fig. A3 Transient emission factors of CO_2, CO, and VOCs from the smouldering of different fuels at a low airflow velocity of 4 mm/s and a high airflow velocity of 18 mm/s. Mean of mass flux (line with symbol) and values of range (cloud) from the repeated experiments are shown.